



## A FUZZY BASED INFERIOR ALVEOLAR NERVE CANAL DETECTION IN PANORAMIC CBCT IMAGES

S. Mohamed Mansoor Roomi<sup>1\*</sup>, P. Uma Maheswari<sup>2</sup>, V S Lokesh<sup>3</sup>, B T Shreya<sup>4</sup>

### Abstract

Inferior Alveolar Nerve canal(IAC) is most sensitive nerve canal and it should be avoided during the surgery of impacted wisdom tooth and applications like dental implants and detection of IAC plays an important role in dental surgery. This paper proposes an automated approach for detection of IAC in the mandibular region, which is vital for Oral and Maxillofacial surgery. The proposed algorithm comprises Contrast-Limited Adaptive Histogram Equalization (CLAHE) to improve the visibility of the input image. The B-Spline method is used to disconnect the upper and lower jaws, and Vertical Integral Projection is used to divide the lower jaw into two sections. Fuzzy Inference system for edge detection is used to extract the far range of edges from the segmented preprocessed image. BRISK (Binary Robust Invariant Scalable Key points) feature descriptor is used to detect feature point location of the nerve canal from Edge detected image. Then the locations of the points are connected and the IAC is detected using curve fitting approach. This algorithm provides better results compared with ground truth image and it has an ability to detect the alveolar nerve canal successfully.

**Index Terms:** Inferior Alveolar Nerve Canal, B-Spline, Fuzzy Inference System, BRISK.

<sup>1</sup>\*Department of ECE, Thiagarajar College of Engineering, Madurai. Email: smmroomi@tce.edu

<sup>2</sup>Department of IT, Velammal College of Engineering and Technology, Madurai.

Email: umamahes.p@gmail.com

<sup>3</sup>Department of ECE, Thiagarajar College of Engineering, Madurai. Email: vslokes10@gmail.com

<sup>4</sup>Department of ECE, Thiagarajar College of Engineering, Madurai. Email: beetee0604@gmail.com

**\*Corresponding Author:** S. Mohamed Mansoor Roomi

\*Department of ECE, Thiagarajar College of Engineering, Madurai. Email: smmroomi@tce.edu

**DOI:** 10.48047/ecb/2023.12.si5a.0274

## I. INTRODUCTION

One popular and recognized surgical procedure is dental implantology, which involves inserting a false root in the mandibular area of the jawbone to support a dental prosthesis. The Inferior Alveolar Nerve Canal (IAC), shown in Fig. 1, is one of the largest sensory nerves in the mandibular area. It supplies sensation to molar, premolar teeth, alveolar bone, periodontal membrane and gingivae in the mandible region. Since the position of IAN is in critical anatomic structure, it is most challenging task to avoid the nerve damage during the surgery.

Depending on the stage of surgery intraoperative and postoperative factors causing IAN damage can be divided into two categories. Mechanical, thermal, and toxic variables are categorised as the main causes of IAN injury intraoperatively. The mechanical causes causing IAN injury include the surgical removal of the lower third molar, dental implants, partial or complete resection, compression, encroachment, scalpel, stretching, or deep cut brought on by block anaesthesia [1][2][3]. Damage to the IAN can result in altered sensation, which can cause paresthesia, dysesthesia, or anaesthesia as well as persistent neuropathic pain. [4][5][6]. In a research involving 90 patients, the removal of the third molar was found to be responsible for 60% of the IAN damage, followed by local anaesthesia (19%), implant surgery (18%), and endodontic issues (8%). The IAN damage stops facial nerves, especially those in the chin and lip, from regenerating. Therefore, it is essential to prevent damaging the IAN canal and the lower third molar's root when performing oral and maxillofacial surgery.

An expert system is required to delineate the IAN because it is challenging to differentiate it from other soft tissue. To better understand how to segment the IAN, the expert system can be created with the aid of image processing techniques. In order to prevent injury in IAN, Thangavelu et al. showed the location of the foramen in the mandibular region from various anatomical landmarks [8].

Sotthivirat and Narkbuakaew [9] suggested a method for canal identification in a panoramic X-ray image that is morphologically based. However, this method does not offer the entire anatomy of the nerve canal. A volume rendering technique-based automated extraction of the IAN has been made available by G. Kim et al. [10]. The best results are obtained by accurately and automatically identifying IAC using the volume

rendering method, but this technique fails if a sizable portion of IAC is missing in the CT image, which is frequently caused by mandibular osteoporosis. Identification of foramen determines how accurately an IAN can be found. Incorrect foramen detection makes the algorithm prone to mistakes, which could lead to the dentist being misled during surgery and severe complications from IAN damage. Therefore, using an automated method to precisely find the IAC is essential for helping the dentist in a better and simpler manner.

This paper proposes algorithm for locating the IAC automatically and accurately to reduce the risk factors during the surgery. The proposed work comprises of pre-processing to enhance the image with high precision, localization for detecting the position of IAC properly and segmentation to extract the IAC from CT image. Evaluation of segmentation accuracy is done by analyzing texture feature of IAC and path detection error.

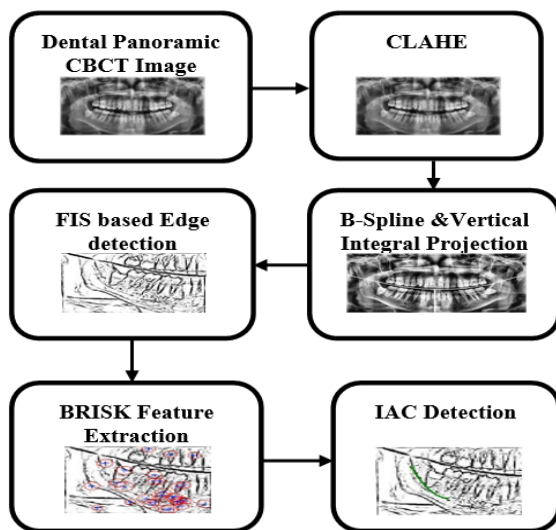
The rest of this paper is structured is as follows: Section 2 interprets the methodology for detecting the IAC accurately. Section 3 deals with experimental results and discussion and the paper is concluded in section 4.

## II. METHODOLOGY

For the purpose of extracting the inferior alveolar nerve canal, the panoramic CT image is used as the input (IAC). This study uses CLAHE for pre-processing in order to enhance the nerve region in the input image [11]. The output of the pre-processing is then given to the B-spline, which enhances the image with good visual interpretation because it includes uniform distribution of pixel grey levels [12]. B-splines are used to divide the upper and lower jaws, vertical integral projection divides the lower mandible into two halves, and edge detection is based on a fuzzy inference system. The edge identified image's Binary Robust Invariant Scalable Key points (BRISK) feature is used to extract the IAC's invariant points. The curve fitting polynomial function is used to integrate the IAC feature points.

### A. Contrast Limited Adaptive Histogram Equalization

CLAHE is used to increase local contrast in CT images. In an image designated a block, CLAHE is carried out in discrete areas. CLAHE limits the slope associated with the input image's grey level in order to prevent saturation in an image.

**Fig. 2** Pipeline of the Proposed Work

Only the maximum number of pixels is allowed in each local histogram bin during this process. To maintain the same overall histogram count after clipping the histogram, the clipped pixels are evenly redistributed throughout the entire histogram [11].

### B. B-Spline & Vertical Integral Projection

B-Spline has a significant degree of freedom in curve design and can change the shape of curves using control points. A collection of knots and a set of parameters for each check point must be considered when designing a B-spline curve. Local maxima in the vertical and horizontal projections are used as the control point coefficient. An image function's vertical projection (Projection(y))  $I(x,y)$  is the total pixel intensity for each column, with width and height ranging from 0 to 1 for both. A graph of integral intensity is created by the sequence of projections ( $y_0$ ), ( $y_1$ ), and ( $y_{H-1}$ ) [13]. The definition of vertical and horizontal projection is

$$\text{Projection}(y) = \sum_{x=0}^w I(x, y) \quad (1)$$

$$\text{Projection}(x) = \sum_{y=0}^w I(x, y) \quad (2)$$

The set U is a knot vector and knot span is taken as 10.

$$U = \{u_0, u_1, u_2, \dots, u_m\} \quad (3)$$

The composite curve will be generated by joining all of the knot points, dividing the image into two areas. By adding up all the intensities along the vertical axis, the vertical integral projection divides the lower mandible into two parts. The B-

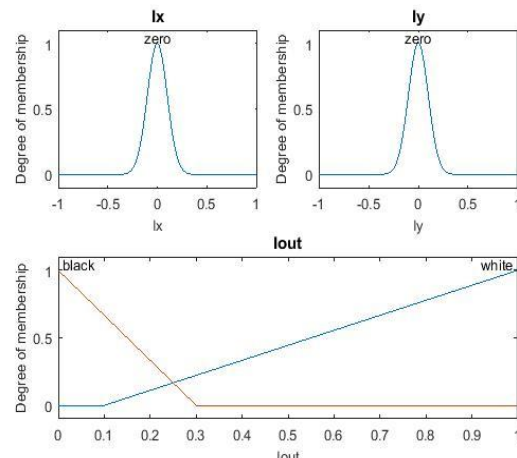
Spline curve's centre coordinate value is considered to be a vertical spot.

### C. Fuzzy Inference System based Edge Detection

Fuzzy Inference system uses membership function to define the degree to which a pixel belongs to an edge [14]. For detecting the edge, Gradient is calculated along x ( $G_x = [0 \ 0.35]$ ) and y direction ( $G_y = G_x'$ ) and it is convolved with the ROI of the projected image. Gaussian membership function with zero mean and standard deviation with the value of 0.1 is specified for each convolved image. Variance is also added with the membership function in the range of [0 1]. If the pixel gradient value is zero, then it belongs to zero membership function with a degree of 1. Triangular membership function with triplets is defined for influencing the detected edges and it is shown in Fig 3.

For detecting the edges rule is added in such a way that a pixel is white when it belongs to a uniform region otherwise it is black and it is shown below

$$\begin{aligned} I_{out} = 1 & \quad I_x = 0 \text{ and } I_y = 0 \\ I_{out} = 0 & \quad I_x \neq 0 \text{ and } I_y \neq 0 \end{aligned} \quad (4)$$

**Fig 3.** Triangular Membership Function

### D. BRISK Feature Extraction

Binary Robust Invariant Scalable Key points detecting robust invariant feature using following steps.

- Scale space representation for octave and intra octave image using down sampling.
- Corner detection and key point detection using FAST score

The maximum value is selected as a feature point with orientation and scale after being calculated

and interpolated using a 1D quadratic function over the scale space.

#### E. IAC Detection using Polynomial Curve Fitting

Curve fitting is the process of creating a curve that, potentially subject to constraints, has the greatest fit to a set of data points [15]. IAC is identified using a 2nd order polynomial function with the coordinates of a feature point and a rotation value, and it is described as

$$f(x) = p_1x^2 + p_2x + p_3 \quad (5)$$

Where  $p_1 = -0.02436, p_2 = 5.636, p_3 = -185.7$  is chosen for left side IAC detection and  $p_1 = -0.01112, p_2 = 4.541, p_3 = -203.9$  is chosen for right side IAC detection and feature point coordinate value is given as  $x$ .

### III. RESULTS AND DISCUSSION

Dental Panoramic CT image is taken as input is shown in Fig 4a and the algorithm is developed using MATLAB. Enhanced image using CLAHE is shown in Fig 4b. It enhances the input image by transforming the intensity values. Since it operates on the small region in an image, artificial induced boundaries and amplifying noise are eliminated.



**Fig 4a.** Panoramic CT image



**Fig 4b.** Preprocessed Image (CLAHE)

The lower mandible is isolated from the preprocessed image using B-spline segmentation, as shown in Fig. 4c. It enables local control over the spline curve's shape to achieve a smoother curve and its completely accurate splitting of the image into its two halves using local minimum points.



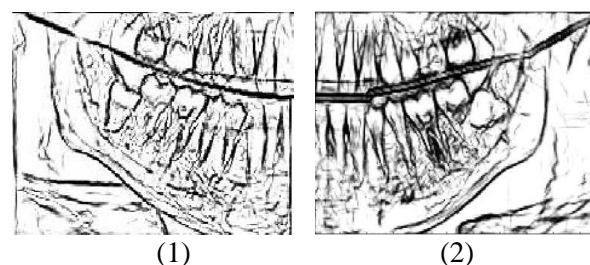
**Fig 4c.** B-Spline Curve

Figure 4d shows how the vertical integral projection divides the lower jaw into two parts by adding up all the intensities along the vertical direction.



**Fig 4d.** Vertical Integral Projection

The region of interest is taken from the projected image, by matching the steepest descent values in x and y directions identifies edges in an image using FIS and it is shown in Fig 4e (1) (2) for both left and right side. Binary Robust Invariant Scalable Keypoints detects multiscale corner feature and it is depicted in Fig 4f (1) (2). IAC have different orientation compared to other regions in an image. Using feature points coordinates and orientation the curve is detected in the CT image is shown green colour in Fig 4g (1) (2). Comparing IAC detected image with the ground truth image gives 89% of accuracy.



**Fig 4e.** Edge Detection using FIS (1) Left Side (2) Right Side

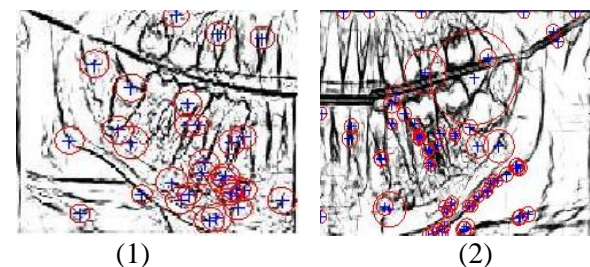


**Fig 4f.** BRISK Feature Extraction (1) Left Side (2) Right Side

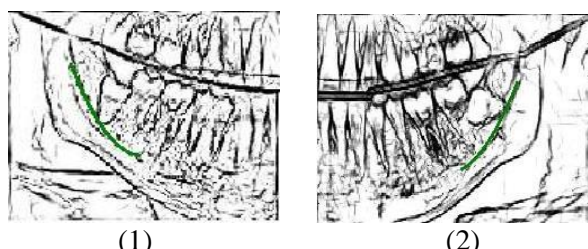


**Fig 4g.** IAC detection (1) Left Side (2) Right Side

#### IV. CONCLUSION

In this paper, a fuzzy based edge detection and BRISK feature extraction is proposed for detecting IAC accurately. This will be helpful at the time of Oral and Maxillofacial surgery and reduce the risk factors during the surgery. Fuzzy Inference System and BRISK feature extraction produces satisfying result and the accuracy is improved. After analysing with the ground truth image, it is observed that this algorithm provides automatic, less complex and 89% of accurate results.

#### REFERENCES

1. Yooseok Shin, Byoung-Duck Roh, Yemi Kim, Taehyeon Kim, Hyungjun Kim, "Accidental injury of the inferior alveolar nerve due to the extrusion of calcium hydroxide in endodontic treatment: a case report", Restorative Dentistry and Endodontics, ISSN 2234-7666, 2016.
2. Dr. Nicola Mahon, Prof. Leo FA Stassen, "Post-extraction inferior alveolar nerve neurosensory disturbances- A guide to their evaluation and practical management", Journal of the Irish Dental Association, Volume 60(5), pp. 241-250, 2014.
3. Juan F Martine-Lage Azorin, Gustavo Segura Andres, Rosa P Valenzuela Molina, Carlos Almendro Muries and Ruben Agustin Panadero, "Prevention and Treatment of IAN Injuries: A Literature Review," JBR Journal of Interdisciplinary Medicine and Dental Science, vol.2, Issue 3.1000123, ISSN:2376-032X, 2014.
4. [www.agd.org/generaldentistry](http://www.agd.org/generaldentistry)
5. Ahmed Ali Alhassani, Ali Saad Thafeed Al Ghamdi, "Inferior Alveolar Nerve Injury in Implant Dentistry: Diagnosis, Causes, Prevention, and Management," Journal of Oral Implantology, vol. XXXVI, No. Five, pp. 401–406, 2010.
6. Rachele Censi, Virna Vavassori, Andrea Enrico Borgonovo, and Dino Re, "Infection Related Inferior Alveolar Nerve Paresthesia in the Lower Premolar Teeth," JBR Journal of Interdisciplinary Medicine and Dental Science, vol.2, Issue 3.1000123, ISSN:2376-032X, 2014.
7. Renton T, Yilmaz Z , "Profiling of patients presenting with posttraumatic neuropathy of the trigeminal nerve", J Orofac Pain 25:333-344.
8. K. Thangavelu, R. Kannan, N. Senthil Kumar, E. Rethish, S. Sabitha, N. Sayeeganesh, "Significance of localization of mandibular foramen in an inferior alveolar nerve block", Journal of Natural Science, Biology and Medicine, Vol 3, Issue 2, pp. 156-160, Feb 2016.
9. S. Sothivirat and W. Narkbuakaew, "Automatic detection of inferior alveolar nerve canals on CT images," in Proc. IEEE Trans. Biomed. Circuits Syst., 2006, pp. 142–145.
10. G. Kim et al., "Automatic extraction of inferior alveolar nerve canal using feature-enhancing panoramic volume rendering". IEEE Transactions on Biomedical Engineering, 58(2):253–264, Feb 2011.
11. Rajesh Garg, Bhawna Mittal, Sheetal Garg, "Histogram Equalization Techniques for Image Enhancement," IJECT Vol.2.Issue 1,March 2011.
12. Pandyan, U.M., Arumugam, B., Gurunathan, U. et al. Automatic localization of inferior alveolar nerve canal in panoramic dental images. SIViP **16**, 1389–1397 (2022). <https://doi.org/10.1007/s11760-021-02091-1>
13. Rafael C. Gonzalez, Richard E. Woods, Steven L. Eddins, Digital Image Processing using MATLAB, Second Edition, McGraw-Hill, 2010.
14. <http://in.mathworks.com/help/fuzzy/examples/fuzzy-logic-image-processing.html>
15. <https://in.mathworks.com/products/curvefittin g.html>